UNIVERSITY
OF WOLLONGONG
AUSTRALIA

University of Wollongong
Research Online

Faculty of Engineering and Information Sciences - Papers: Part A

Faculty of Engineering and Information Sciences

2012

Wearable sensors in intelligent clothing for measuring human body temperature based on optical fiber Bragg grating

Hongqiang Li
Tianjin Polytechnic University

Haijiang Yang
Tianjin University of Technology

Enbang Li
University of Wollongong, enbang@uow.edu.au

Zhihui Liu
Tianjin Polytechnic University

Kejia Wei
Tianjin Polytechnic University

Publication Details

H. Li, H. Yang, E. Li, Z. Liu & K. Wei, "Wearable sensors in intelligent clothing for measuring human body temperature based on optical fiber Bragg grating," Optics Express, vol. 20, (11) pp. 11740-11752, 2012.

Research Online is the open access institutional repository for the University of Wollongong. For further information contact the UOW Library: research-pubs@uow.edu.au

Wearable sensors in intelligent clothing for measuring human body temperature based on optical fiber Bragg grating

Abstract
Measuring body temperature is considerably important to physiological studies as well as clinical investigations. In recent years, numerous observations have been reported and various methods of measurement have been employed. The present paper introduces a novel wearable sensor in intelligent clothing for human body temperature measurement. The objective is the integration of optical fiber Bragg grating (FBG)-based sensors into functional textiles to extend the capabilities of wearable solutions for body temperature monitoring. In addition, the temperature sensitivity is 150 pm/°C, which is almost 15 times higher than that of a bare FBG. This study combines large and small pipes during fabrication to implant FBG sensors into the fabric. The law of energy conservation of the human body is considered in determining heat transfer between the body and its clothing. The mathematical model of heat transmission between the body and clothed FBG sensors is studied, and the steady-state thermal analysis is presented. The simulation results show the capability of the material to correct the actual body temperature. Based on the skin temperature obtained by the weighted average method, this paper presents the five points weighted coefficients model using both sides of the chest, armpits, and the upper back for the intelligent clothing. The weighted coefficients of 0.0826 for the left chest, 0.3706 for the left armpit, 0.3706 for the right armpit, 0.0936 for the upper back, and 0.0826 for the right chest were obtained using Cramer's Rule. Using the weighting coefficient, the deviation of the experimental result was ± 0.18°C, which favors the use for clinical armpit temperature monitoring. Moreover, in special cases when several FBG sensors are broken, the weighted coefficients of the other sensors could be changed to obtain accurate body temperature.

Keywords
clothing, temperature, intelligent, body, human, measuring, wearable, sensors, grating, bragg, fiber, optical

Disciplines
Engineering | Science and Technology Studies

Publication Details
H. Li, H. Yang, E. Li, Z. Liu & K. Wei, "Wearable sensors in intelligent clothing for measuring human body temperature based on optical fiber Bragg grating," Optics Express, vol. 20, (11) pp. 11740-11752, 2012.

This journal article is available at Research Online: http://ro.uow.edu.au/eispapers/298

Wearable sensors in intelligent clothing for measuring human body temperature based on optical fiber Bragg grating

Hongqiang Li,[1,*] Haijing Yang,[2] Enbang Li,[3] Zhihui Liu,[1] and Kejia Wei[1]

[1]*School of Electronics and Information Engineering, Tianjin Polytechnic University, Tianjin 300387, China*
[2]*Library, Tianjin University of Technology, Tianjin 300384, China*
[3]*School of Electrical, Computer and Telecommunications Engineering, University of Wollongong, Wollongong, NSW2522, Australia*
**lihongqiang@tjpu.edu.cn*

Abstract: Measuring body temperature is considerably important to physiological studies as well as clinical investigations. In recent years, numerous observations have been reported and various methods of measurement have been employed. The present paper introduces a novel wearable sensor in intelligent clothing for human body temperature measurement. The objective is the integration of optical fiber Bragg grating (FBG)-based sensors into functional textiles to extend the capabilities of wearable solutions for body temperature monitoring. In addition, the temperature sensitivity is 150 pm/°C, which is almost 15 times higher than that of a bare FBG. This study combines large and small pipes during fabrication to implant FBG sensors into the fabric. The law of energy conservation of the human body is considered in determining heat transfer between the body and its clothing. The mathematical model of heat transmission between the body and clothed FBG sensors is studied, and the steady-state thermal analysis is presented. The simulation results show the capability of the material to correct the actual body temperature. Based on the skin temperature obtained by the weighted average method, this paper presents the five points weighted coefficients model using both sides of the chest, armpits, and the upper back for the intelligent clothing. The weighted coefficients of 0.0826 for the left chest, 0.3706 for the left armpit, 0.3706 for the right armpit, 0.0936 for the upper back, and 0.0826 for the right chest were obtained using Cramer's Rule. Using the weighting coefficient, the deviation of the experimental result was ± 0.18°C, which favors the use for clinical armpit temperature monitoring. Moreover, in special cases when several FBG sensors are broken, the weighted coefficients of the other sensors could be changed to obtain accurate body temperature.

© 2012 Optical Society of America

OCIS codes: (060.3735) Fiber Bragg gratings; (060.2300) Fiber measurements; (080.2720) Mathematical methods (general).

References and links

1. D. Karalekas, "On the use of FBG sensors for measurement of curing strains in photocurable resins," Rapid Prototyping J. **14**(2), 81–86 (2008).
2. K. O. Hill and G. Meltz, "Fiber Bragg grating technology fundamentals and overview," J. Lightwave Technol. **15**(8), 1263–1276 (1997).
3. A. Othonos, "Fiber Bragg gratings," Rev. Sci. Instrum. **68**(12), 4309–4341 (1997).
4. J. L. Zheng, R. Wang, T. Pu, L. Lu, T. Fang, Y. Su, L. Li, and X. F. Chen, "Phase-controlled superimposed FBGs and their applications in spectral-phase en/decoding," Opt. Express **19**(9), 8580–8595 (2011).
5. P. Gould, "Textiles gain intelligence," Mater. Today **6**(10), 38–43 (2003).
6. N. Butler, "Latest developments and trends in intelligent clothing revealed," Tech. Text. Int. **14**(7–8), 31–36 (2005).

#164653 - $15.00 USD Received 14 Mar 2012; revised 30 Apr 2012; accepted 3 May 2012; published 9 May 2012
(C) 2012 OSA

7. A. P. J. Hum, "Fabric area network -a new wireless communications infrastructure to enable ubiquitous networking and sensing on intelligent clothing," Comput. Netw. **35**(4), 391–399 (2001).
8. L. Li, W. M. Au, Y. Li, K. M. Wan, W. Y. Chung, and K. S. Wong, "A novel design method for an intelligent clothing based on garment design and knitting," Text. Res. J. **79**(18), 1670–1679 (2009).
9. J. B. Lee and V. Subramanian, "Weave patterned organic transistors on fiber for e-textiles," IEEE Trans. Electron. Dev. **52**(2), 269–275 (2005).
10. J. Witt, F. Narbonneau, M. Schukar, K. Krebber, J. De Jonckheere, M. Jeanne, and D. Kinet, B. paquet, A. Depré, L.T. D'Angelo, T. Thiel, and R. Logier, "Medical textiles with embedded fiber optic sensors for monitoring of respiratory movement," IEEE Sens. J. **12**(1), 246–254 (2012).
11. A. Grillet, D. Kinet, J. Witt, M. Schukar, K. Krebber, F. Pirotte, and A. Depré, "Optical fiber sensors embedded into medical textile for healthcare monitoring," IEEE Sens. J. **8**(7), 1215–1222 (2008).
12. L. T. D'Angelo, S. Weber, Y. Honda, T. Thiel, F. Narbonneau, and T. C. Luth, "A system for respiratory motion detection using optical fibers embedded into textiles," in Engineering in Medicine and Biology Society EMBS'08 Annual International Conference of the IEEE (2008), pp. 3694–3697.
13. J.-R. Chen, J.-M. Tseng, Y.-F. Lin, S.-Y. S. Wang, and C.-M. Shu, "Adiabatic runaway studies for methyl ethyl ketone peroxide with inorganic acids by vent sizing package 2," Korean J. Chem. Eng. **25**(3), 419–422 (2008).
14. M. Sund-Levander, C. Forsberg, and L. K. Wahren, "Normal oral, rectal, tympanic and axillary body temperature in adult men and women: a systematic literature review," Scand. J. Caring Sci. **16**(2), 122–128 (2002).
15. R. Nielsen and B. Nielsen, "Measurement of mean skin temperature of clothed persons in cool environments," Eur. J. Appl. Physiol. Occup. Physiol. **53**(3), 231–236 (1984).

1. Introduction

A fiber Bragg grating (FBG) is a type of distributed Bragg reflector constructed in a short segment of optical fiber that reflects particular wavelengths of light and transmits all the others. This reflection is achieved by adding a periodic variation to the refractive index of the fiber core, which generates a wavelength-specific dielectric mirror. Therefore, the FBG can be used as an inline optical filter to block certain wavelengths, or as a wavelength-specific reflector [1]. Recently, fiber Bragg gating sensors have demonstrated great advantage over electronic sensors for applications in intelligent structures, civil engineering, harsh environments, built health monitoring system and so on [2–4].

Intelligent clothing is the integration and intersection of electronic information, material, textile, and other related subjects. Such clothing is sensitive and can respond to environmental conditions and other factors; not only can it sense changes of both the environment outside and conditions inside the human body, it can also respond to these changes through a feedback mechanism in a timely manner. The features of intelligent clothing are portable, easy monitoring in real-time, and so on. Sensing, feedback, and reaction are its three essential factors [5,6]. A lot of achievements have been obtained in the research of intelligent clothing. In [7], a new wireless communication infrastructure to enable networking and sensing on clothing is proposed, also the architecture and technology of the fabric area network (FAN) is described. This technology proved to be emission-safe, low-cost and easy to maintain. In [8], garment design method is proposed for a specific task based on combinations of garment design and knitting technology to provide the required confining pressure, electrical and mechanical properties for the intelligent clothing. Experiments revealed that problems faced in intelligent clothing design, such as confining pressure, flexible electronic circuitry, and so on, could be successfully solved by the use of this method and can be applied in the future design of intelligent clothing. In [9], devices are defined and positioned solely by a weaving pattern, meaning that simple circuits could potentially be directly built into fabric during manufacturing which offers a novel approach for providing information routing within fabric and a major hurdle in electronic textile development. Perception, feedback and reaction are three elements of intelligent clothing. But in fact the conductive fiber and the cotton fiber blend together, which leads to the realization of receiving data from the embedded sensor. And the data can be transformed to a special receiver with the size of a credit card. This receiver can be put at the waist, can store information, and then indicate it on the mobile phone, family personal computer or wrist monitors, in order to monitor the important life characteristics of certain person, issuing a warning signal in time. According to the example

#164653 - $15.00 USD Received 14 Mar 2012; revised 30 Apr 2012; accepted 3 May 2012; published 9 May 2012
(C) 2012 OSA

mentioned above, the conductive fiber and the cotton fiber blend together, the receiver of the intelligent clothing just has the size of a credit card, can be put at the waist, being used to store, monitor and send out signal. So the sensing of intelligent clothing has advantages such as convenience, accuracy, and feasibility. Being small, portable, compatible to yarn, and easy to weave into textiles, FBG sensors have become the most promising material of sensing element in forming intelligent clothing.

Numerous diseases have fever as one of the early symptoms. Fever can be classified into two kinds. One is non-infectious fever, which occurs in cases such as in immunological diseases, tumors, and metabolic diseases. Among them, tumors are the greatest killers of human beings. The other kind is infectious fever, such as the H5N1 highly pathogenic avian influenza and Severe Acute Respiratory Syndromes (SARS), both of which have caused global panic in recent years. Thus, measurement of human body temperature is significant in the early detection of diseases, timely diagnosis, and treatment.

This paper aims to investigate key problems of intelligent clothing for temperature measurement. Mainly, the focus is on the theories and methods of measuring human body temperature through distributed optical FBG in intelligent clothing. Then, a mathematical model of human body temperature is built, and ways to weave optical FBG sensors into the fabric are determined. Intelligent clothing can monitor, process, store, and provide data on human body temperature in real-time. In addition, among other benefits, such clothing is portable, affordable, and accurate in measurement. Moreover, continuous data of the patient's body temperature changes can be provided for doctors and nurses, thereby allowing for correlation analysis by combining these data with other physical parameters. Thus, intelligent clothing can contribute to the timely detection of infection, tumors, and other diseases, such as SARS and the Avian Influenza. Furthermore, safe and accurate tele-monitoring of patients can be achieved, helping ensure that patients are treated in a timely manner [10–12] This achievement is significant and possesses great application value in promoting people's health, especially that of old people and children who lack the ability of language expression.

2. FBG fabrication and embedment

2.1 Polymer package for FBG sensors

A bare FBG has very low temperature sensitivity of 10 pm/°C at about 1,550 nm in wavelength. Thus, improving the temperature sensitivity of FBG will contribute enhanced precision. A novel FBG temperature sensor based on an FBG partly embedded in a polymer-filled strip is designed in this paper.

Figure 1 illustrates the configuration of the proposed temperature sensor. All the FBGs are embedded in a rectangle package with length, width, and thickness of 25, 8, and 3 mm, respectively. According to Fig. 1, inject polymer which is mixed evenly into two long strip model with length, after long time curing, two long strip polymer received. Grind a groove in the center of the polymer with fine sandpaper, polish smooth, and then put the bare FBG in the groove. Finally, fix and paste on the both side of the FBG until the structure is cured and taken shape. During the packaging process, the FBG is imposed a certain degree of prestressing to avoid the nonlinear and the distortion of the reflection wavelength shift date, which is caused by the chirp of the FBG. Fix FBG at both side of the substrate to make sure that the FBG located in the center of the substrate material and parallel to the base material, As a result, not only the good linear relationship between the FBG wavelength and the temperature is ensured, but also the stability of the sensor structure. In order to eliminate the effect of unstable force field on FBG, we add certain pretension on fiber Bragg grating in the process of encapsulation. In this way, the FBG is in a tension state and therefore a stable space position and force relation is always existed between the FBG and the substrate. So when we did the temperature experiment, the temperature character of FBG is stable.

#164653 - $15.00 USD Received 14 Mar 2012; revised 30 Apr 2012; accepted 3 May 2012; published 9 May 2012
(C) 2012 OSA

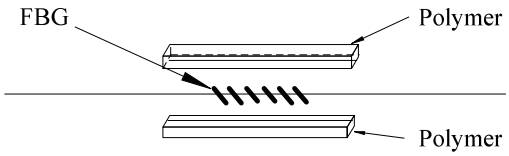

Fig. 1. Sketch of polymer package for FBG.

The polymer used is the copolymerization of unsaturated polyester resin mixtures containing 5.0 wt% Methyl Ethyl Ketone Peroxide (MEKP) and 2.0 wt% cobalt naphthenate at 25 °C. Unsaturated polyester resins are produced by the polycondensation of saturated and unsaturated dicarboxylic acids with glycols. Such resins form highly durable structures and coatings when cross-linked with a vinylic reactive monomer, most commonly styrene. Their properties depend on the types of acids and glycols used and their relative proportions. MEKP is highly explosive, similar to acetone organic peroxide, but is slightly less sensitive to shock and temperature as well as more stable in storage [13] Cobalt naphthenate is a mixture of the cobalt derivatives of naphthenic acids; it is widely employed as catalyst because of its solubility in nonpolar substrates. Naphthenates, which are mixtures, help confer high solubility. The second benefit of these species is their low cost. A well-defined compound that exhibits many of the properties of cobalt naphthenate is the cobalt complex of 2-ethylhexanoic acid. According to technical literature, naphthenates are described as salts, but they are probably also non-ionic coordination complexes with structures similar to that of basic zinc acetate.

We use the method of curve (in Fig. 2) fitting calculated the temperature sensitivity of the FBG is 150pm/°C. As shown in 2, with the polymer, the FBG's temperature sensitivity is 150 pm/°C, which is almost 15 times higher than that of a bare FBG. Figure 3 shows the spectrum of polymer-packaged FBG sensors.

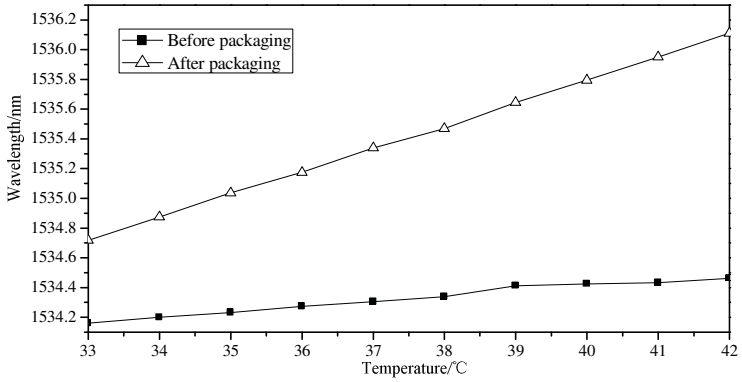

Fig. 2. Wavelength increment and temperature for polymer-packaged FBG sensors and bare FBG sensors.

#164653 - $15.00 USD Received 14 Mar 2012; revised 30 Apr 2012; accepted 3 May 2012; published 9 May 2012
(C) 2012 OSA

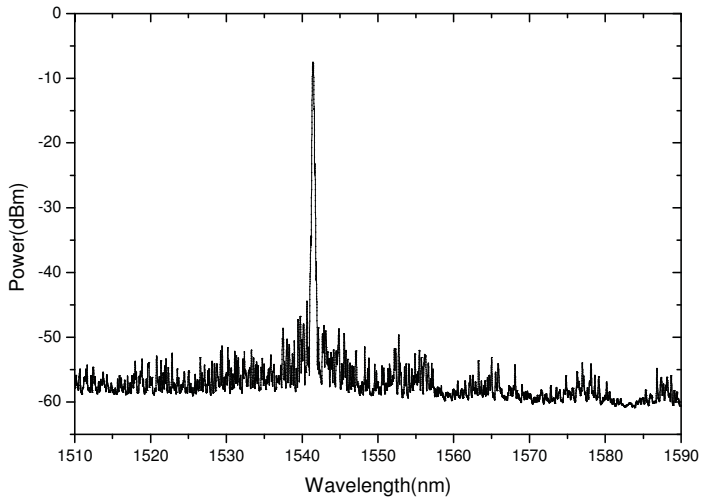

Fig. 3. Spectrum of polymer-packaged FBG sensors.

2.2 Embedment of FBG sensors into fabric

FBG sensors can be embedded into textile fabrics. The textile substrates could be woven, non-woven, or knitted fabrics. In incorporating the optical fiber sensors, non-woven fabrics have the advantage of a very large surface area because of the presence of small-sized fibers. Moreover, the levels of mechanical stresses involved in the incorporation of optical fiber sensors in non-woven fabrics are much lower than those in the case of woven or knitted fabrics, thereby leading to less fiber breakages, especially when silica optical fibers are used.

The FBG sensors are embedded into the fabric by combining large and small pipes together in fabrication, while keeping optical fiber and sensors complete, unbent, and harmonious with the activities of fabric warp and filling. During the manufacturing process, the clothing is divided into several blocks to weave and implant the sensors in the corresponding place, to keep pipes in their exact places, and to prevent them from being destroyed. After the sensors are implanted, the chain draft of weaving is changed so that the sensors will remain in place within the pipes and not move around. When all of the weaving is completed, the blocks are sewn together.

By using large and small pipes together in the fabrication method, we divide fabric into three parts. The first part is manufactured by plain weave. The second part is manufactured by tubular tissues and plain weave, as a part to implement large pipe. The third part uses the structure of small pipes covered by large pipes. When we manufacture the third part, we keep the pipe orifice open to form a cylindrical hollow bag, implant FBG sensors into it, and change the chain draft. Then we can continue to fabricate the second part and the first part to finish encapsulating FBG sensors into fabric.

The completed fabric is shown in Fig. 4, which adopts the implanting method of covering small pipe with large one to form a cylindrical hollow bag, and fulfill the consistency between activities of warp weave and filling weave without influencing the outward appearance of the fabric.

For the experiment on the FBG temperature measurement, a light path and demodulation circuit is built based on the Fabry-Perot (F-P) tunable filter. The FFP –TF2 filters we used are come from American Micron Optics Ics. The tuning range is 1520-1570 nm, the tuning speed is 5 Hz, and the tuning voltage is 0-10V, which is ideal for low cost, high volume applications and low power requirements. As Fig. 5 shows, under the control of the output drive voltage and the tunable narrow-band light source, which is composed of a broadband light source SLED, isolators, and F-P filters in optical path demodulator, different center wavelengths of

#164653 - $15.00 USD Received 14 Mar 2012; revised 30 Apr 2012; accepted 3 May 2012; published 9 May 2012
(C) 2012 OSA

the narrow-band light are exported; these enter into the sensitive passage through a coupler. After passing through the photoelectric detector, the reflected light of the FBG sensors, which are implanted in the intelligent clothing, turns off the electrical signals, commencing the analysis of the wavelength after sampling in the signal processing.

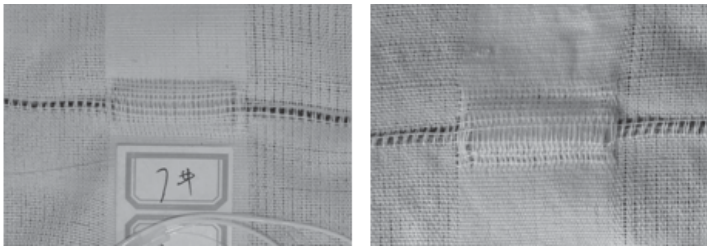

(a) (b)

Fig. 4. Picture of embedment of FBG sensors into fabric, (a) Front side of the fabric, (b) Back side of fabric.

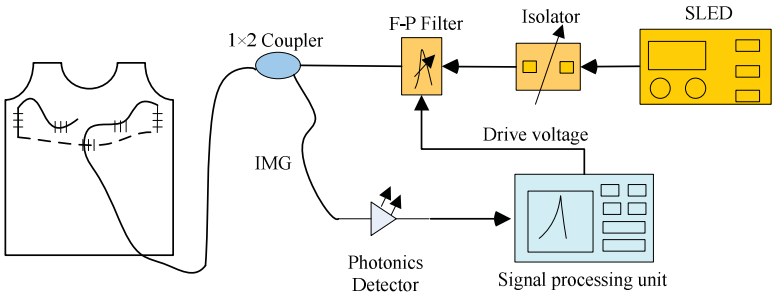

Fig. 5. Schematic diagram of the demodulation system for body temperature measurement in intelligent clothing.

The fiber Bragg grating adopted by this paper is prepared by the phase-mask method, which is one kind of UV-written fiber Bragg grating. The rate of its peak reflectivity is close to 100%. Its side mode suppression ratio is about 29dB. The range of wavelength is 0.4 nm when the bandwidth is 3 dB. The range of wavelength is 0.8 nm when the bandwidth is 30 dB. As shown in Fig. 6, the central wavelength of the five FBGs are respectively 1532.6, 1533.4, 1540.4, 1542.1, and 1548.4 nm. The FBGs' temperature sensitivity are 148.2, 141.5, 146.2, 146.6, and 150.2 pm/°C.

This study uses C8051F060 and LPC2106 to collect and process wavelength signals. C8051F060, which is a microcontroller for data acquisition, includes several key enhancements to the CIP-51 core and its peripherals to improve overall performance and the ease of use in end applications; also included are mixed-signal system-on-a-chip MCUs with 59 digital I/O pins, and two integrated 16-bit 1 Msps ADCs. LPC2106 consists of an ARM7TDMI-S CPU with emulation support, the ARM7 local bus for interface to on-chip memory controllers, the AMBA advanced high-performance bus for interface to the interruption controller, and the VLSI peripheral bus for connection to on-chip peripheral functions. LPC2106 configures the ARM7TDMI-S processor in little-endian byte order. Considering A/D output voltage signal in C8051F060 as the control of the F-P filter drive voltage through photoelectric conversion, the reflected light of FBG is amplified and filtered by the signal conditioning circuit. The output of the signal conditioning circuit is then sampled and stored with the help of C8051F060, followed by the pre-processing of the sampled data before being sent to LPC2106 through the serial port to achieve the core demodulation algorithm, which provides the results of the temperature algorithm.

#164653 - $15.00 USD Received 14 Mar 2012; revised 30 Apr 2012; accepted 3 May 2012; published 9 May 2012
(C) 2012 OSA

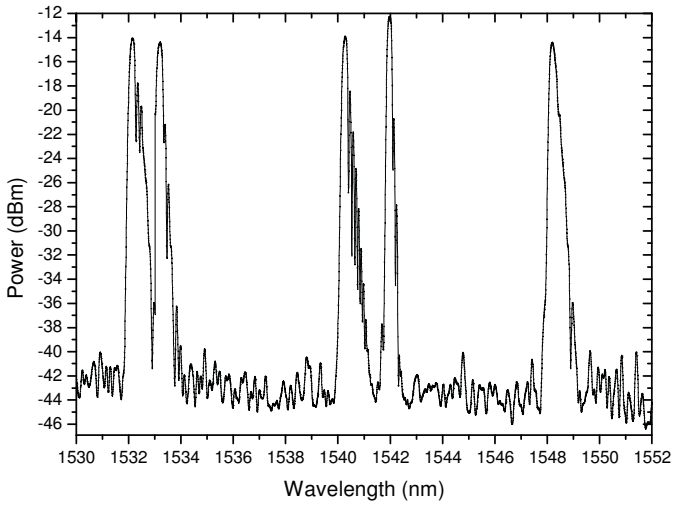

Fig. 6. Spectrum of five series polymer-packaged FBG sensors.

3. Heat transfer mathematical model of FBG sensors

The human body is a heating element. Heat comes from metabolism, and a part of it reaches the surface of human skin by blood circulation, and then spreads to the external environment through microclimate and clothing. When the external temperature is lower than human body temperature, a temperature gradient will occur between the human skin and environment. This leads to heat transmission toward the clothing surface through microclimate and clothing, and then heat spreads to the environment in the form of conduction, convection, and radiation [14]. As FBG sensors, studied and implanted into intelligent clothing, cannot by itself cling to the human body, the physical model of this heat transmission between the human body and FBG sensors is actually the model of body, air layer, and clothing when detecting body temperature, as shown in Fig. 7.

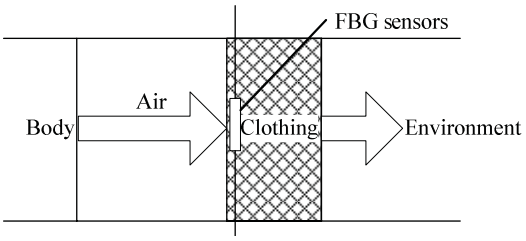

Fig. 7. Heat transmission model between body and clothed FBG sensors.

The constant motion of people, who are in clothing, keep heat transmission in a dynamically changing process. The air under the clothing cannot be completely static. Thus, while the temperature difference between various fabrics results in heat transmission, the movement of air molecules also leads to natural convection. For this reason, this study has chosen tight underclothes during the design of intelligent clothing; the space for air is small enough to stop convection from forming, allowing the study of heat transmission.

The temperature field among the human body, air layer, and clothing changes all the time, making heat transmission a dynamic process. In other words, heat transmission is unstable. Armpit temperature is clinically regarded as body temperature, and the method of its measurement is to dry perspiration under the armpit, place the mercury side of a thermometer deep in the armpit, and bend the patient's arm to keep the thermometer in place at about 5 cm

#164653 - $15.00 USD Received 14 Mar 2012; revised 30 Apr 2012; accepted 3 May 2012; published 9 May 2012
(C) 2012 OSA

higher than the breast. The time spent measuring the temperature is regarded as the time of building a heat balance between the body surface and the thermometer. Afterward, for example, in 3 min, the heat transmission can then be regarded as steady-state heat transmission, which can then be analyzed and examined accordingly.

This paper establishes finite element models of heat transmission among the human body, air layer, and clothing. A cylindrical air element is used with l length l, r radius, and dr thickness from microclimate area. The equivalent heat conductivity is λ, specific heat capacity is c, density is ρ. The λ, c, and ρ are all functions of temperature (T), whereas T is the function of τ, indicating time and r, namely, $\lambda(r, \tau)$, $c(r, \tau)$, $\rho(r, \tau)$. Figure 8 shows the cylindrical element.

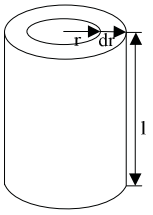

Fig. 8. Strip-shaped micro-cell.

According to the law of energy conservation, for elements during any interval $d\tau$, the heat, including that flowing into the element and that produced by the element itself, is equal to the heat consisting of the heat flowing out of the element and the heat increasing in the element's internal energy. Heat transmission inside the intelligent clothing is only the transmission of heat, and thus, no origins of heat are inside the element. The heat balance is shown as Eq. (1):

$$q_{in} = q_{out} + q_d. \tag{1}$$

where q_{in} is the heat flowing into the element, q_{out} is heat flowing out, and q_d is the heat increasing the element's internal energy.

According to Fourier's law [3,5],

$$q_{in} = -\lambda 2\pi r l \frac{\partial t}{\partial r} d\tau. \tag{2}$$

$$q_{out} = -\lambda 2\pi r \frac{\partial t}{\partial r} - 2\pi\lambda \frac{\partial t}{\partial r} dr - 2\pi\lambda r \frac{\partial^2 t}{\partial r^2} dr - \frac{\partial}{\partial r}[\lambda(r,\tau)]2\pi r \frac{\partial t}{\partial r} dr. \tag{3}$$

$$q_d = 2\pi r l c(r,\tau)\rho(r,\tau)\frac{\partial t}{\partial \tau} d\tau. \tag{4}$$

Substituting Eqs. (2), (3), and (4) into Eq. (1) yields a mathematical model of heat transmission among the human body, air layer, and clothing as Eq. (5):

$$\frac{\partial}{\partial r}[\lambda(r,\tau)]r\frac{\partial t}{\partial r} + \lambda(r,\tau)\frac{\partial t}{\partial r} + \lambda(r,\tau)r\frac{\partial^2 t}{\partial r^2} = c(r,\tau)\rho(r,\tau)r\frac{\partial t}{\partial \tau}. \tag{5}$$

Solving the heat transfer problem, in essence, is solving the differential equations of heat transfer. Additional conditions, called definite conditions, for characterizing the problem are required to obtain the temperature and pressure distribution for the specific heat transfer. For the unstable state heat transfer process, two aspects of definite conditions are required, namely, the initial and boundary conditions of the temperature and pressure distribution. The heat transfer differential equations and definite conditions constitute the complete mathematical description of the heat transfer problem.

#164653 - $15.00 USD Received 14 Mar 2012; revised 30 Apr 2012; accepted 3 May 2012; published 9 May 2012
(C) 2012 OSA

The temperature and pressure distribution in clothing microclimate are initially known, which are the external environment temperature T_a and pressure P_a. Thus, the initial condition is

$$T(r,0) = T_a, p(r,0) = p_a. \tag{6}$$

The internal boundary condition of clothing microclimate is the expression of heat flux on the skin surface, which contains the radiant exothermicity between the skin and the inner surface of the clothing, as well as the heat conduction caused by the temperature gradient. According to the expression of heat flux, the internal boundary condition of heat transmission in microclimate is as follows:

$$-2\pi r\lambda \frac{\partial t}{\partial r} + q_{w1} + q_{bf} = c\rho dv \frac{\partial t}{\partial \tau}. \tag{7}$$

where q_{w1} is the heat flux of the skin surface W/m^2, q_{bf} is the radiant exothermicity between the skin surface and the inner surface of the clothing W/m^2.

The heat transfer from the temperature gradient also occurs at the outer boundary of the clothing microclimate. Hence, the external boundary condition is given by the following:

$$-2\pi r\lambda \frac{\partial t}{\partial r} - q_{w2} = c\rho dv \frac{\partial t}{\partial \tau}. \tag{8}$$

where q_{w2} is the heat flux between the air layer and the external environment W/m^2.

The parameters involved in the clothing microclimate heat transfer model are not constant; they are the variables of the physical parameters of time and temperature changes. The variation of these variables is discussed below with detailed expression.

The thermal conductivity of dry air λ_g is

$$\lambda_g = (2.438714 + 0.7784798\times10^{-2}t - 0.17553068\times10^{-5}t^2)\times10^2.$$

This formula can be applied to temperatures between 0 and 200 °C, whereas the absolute error is less than $0.0156\times10^{-2}\,w/(m.^{\circ}C)$.

The thermal conductivity of the saturated moist air λ_s is

$$\lambda_s = (2.38874 + 0.8798147\times10^{-2}t - 0.1150367\times10^{-3}t^2)\times10^2.$$

This formula can be applied to temperatures between 0 and 90 °C, whereas the absolute error is less than $0.033\times10^{-2}\,w/(m.^{\circ}C)$.

The specific heat of dry air $C_\rho{}^g$ is

$$C_\rho{}^g = 1005.28 - 0.260338\times10^{-1}t + 0.6370071\times10^{-3}t^2.$$

This formula can be applied to temperatures between 0 and 200 °C, and the absolute error is less than $2.5J/(kg.^{\circ}\mathrm{C})$.

The specific heat of the saturated moist air $C_\rho{}^s$ is

$$C_\rho{}^s = 990.56 + 8.75522t - 0.39159t^2 + 0.55695t^3.$$

This formula can be applied to temperatures between 0 and 80 °C; the absolute error is less than $4.2J/(kg.^{\circ}\mathrm{C})$.

The density of dry air ρ^g is

$$\rho^g = 1.2926 - 0.00463t + 1.2619\times10^{-5}t^2.$$

#164653 - $15.00 USD Received 14 Mar 2012; revised 30 Apr 2012; accepted 3 May 2012; published 9 May 2012
(C) 2012 OSA

This formula can be applied to temperatures between −50 and 200 °C, and the absolute error is less than $0.0214 kg / m^3$.

The density of saturated moist air ρ^s is

$$\rho^s = 1.23669 - 0.6238325 \times 10^{-3} t - 0.9965985 \times 10^{-4} t^2.$$

This formula can be applied to temperatures between 0 and 90 °C; the absolute error is less than 0.0.

The microclimate air layer is divided into a finite number of net units using the finite analysis method; afterward, the differential equations in the thermal field are converted to nodal equations, and the temperature of each unit node of the net is generated by numerical calculation [12–14]. The thermal analysis module of the ANSYS finite element software is used to finish the modeling of FBG temperature field in intelligent clothing; this tool reflects the temperature measurement error when the human body wears intelligent clothing.

In the finite element model, 0.5 mm is set as the thickness of the air layer, 2 mm is the thickness of FBG, and 2 mm is the thickness of the cotton fabric, where the thermal conductivity coefficients are 0.027, 0.19, and 1.2 W/m.K under normal conditions, respectively. Figure 9 shows the temperature field model established in this study.

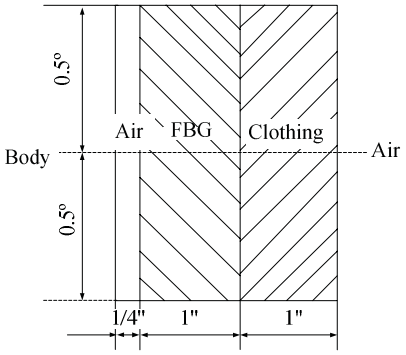

Fig. 9. Temperature finite element model for intelligent clothing.

The study divides the above model into gridding by ANSYS, in which 36 °C is set as the temperature of the body. The range of the temperature of the external environment is 25 °C–35 °C, with a temperature increasing interval of 1 °C. The Choi map will then appear (Fig. 10). The date of the map shows that when the body temperature is constant, the external environment temperature increases by 1 °C, and the FBG-measured temperature will increase by 0.04 °C. The relationship between the change of the external environment temperature and the change of the FBG-measured temperature is then acquire. The body temperature is set to 33 °C–42 °C, with 0.5 °C as increment. The Choi map is produced when the external environment temperature is 25 °C. The date of the map supports the analysis that when the external environment temperature is constant, a smaller difference of the value between the body temperature and the ambient temperature is observed along with the more accurate FBG temperature measurement. During the experiments, temperature deviations can be used in the correction of the FBG temperature measurement as a way of increasing the accuracy of the FBG temperature measurement.

Table 1 presents the correlation analysis between the numerical simulation results of the thermal field and the temperature tested by FBG under stable conditions. The Pearson related coefficient is 0.990, P = 0.000, whereas the relationship between them is a strong positive linear one.

#164653 - $15.00 USD Received 14 Mar 2012; revised 30 Apr 2012; accepted 3 May 2012; published 9 May 2012
(C) 2012 OSA

Table 1. Correlation Analysis of the Temperature Measured by FBG and Simulated by ANSYS

		Measured by FBG	Simulated by ANSYS
Measured by FBG	Pearson Correlation	1	.990(**)
	Sig. (2-tailed)	0	.000
	N	240	240

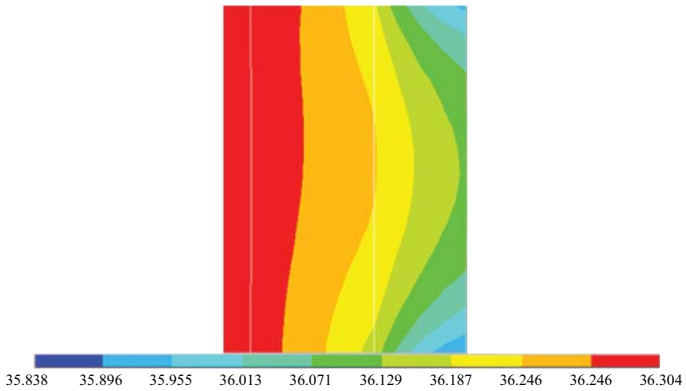

Fig. 10. Predicting temperature distribution in intelligent clothing using ANSYS.

4. Body temperature weighted model of intelligent clothing

To measure human body temperature, optical fiber grating temperature sensors are distributed to five places, namely, left chest, right chest, left armpit, right armpit, and at center of the upper back. As different parts of human body have different temperatures, the data obtained from these five places are not the same. Thus, a weighted model is proposed for the data to derive the final temperature of the human body.

Skin temperature is an important parameter in human physiology. When human beings exchange energy with the environment, skin becomes the interface. The mean skin temperature becomes a significant value in calculating human energy loss as well as in analyzing thermoregulation and other physiological activities. According to the characteristics of dissection, the human body can be divided into several parts with similar dissecting structures and temperature distributions: head, torso, arm, leg, and so on. Subsequently, one or more measuring points can be set on each part, and these temperature data by can be weighed by weighted coefficients from the proportion that these parts occupy in the entire area of the human body. The total score is the human body weighted mean skin temperature (T_s), which can be shown as the following formula:

$$T_s = C_1 T_{s1} + C_2 T_{s2} + \ldots\ldots C_n T_{sn}. \quad (9)$$

In this formula, T_{S1}, T_{S2}, and T_{Sn} represent the temperature of each part in centigrade, and C_1, C_2, and C_n represent the weighted coefficients of each part in the non-dimensional analysis.

The information about skin temperature used in the equations above mostly comes from testees who were naked or wearing single layer under slightly hotter or warm environment. Under such environment, skin vessels were stretching or in normal state, leading to total skin temperature's evenly distributed, so non-weighted method and one point thermometry can work well. However, when people wear thick clothing, especially in cold environment, skin temperature and its distribution will be physiological reaction to the comprehensive function of environmental temperature, clothing, and body activities, and the skin temperature distribution is uneven, so it becomes difficult to get accurate mean skin temperature through a few skin temperature measuring points. Nielsen ever did an experiment on people wearing

#164653 - $15.00 USD Received 14 Mar 2012; revised 30 Apr 2012; accepted 3 May 2012; published 9 May 2012
(C) 2012 OSA

thick clothing at 10 °C [15]. He created thirteen points equation based on Qlesen four-point method, and then selected this as the standard to compare with other eleven weighted equations. The result showed that Teichner six-point method and Ramanathan four-point method all had some differences with the standard skin temperature, only Mitchell twelve-point method, Gagge-Nishi eight-point method and Hardy-Dubios seven-point method had high consistency frequency with the standard skin temperature. In Nielsen's opinion, multipoint weighted method was the best in cold environment.

As the intelligent clothing currently under investigation is mainly for the upper body, this work proposes a new five-point method that is an improvement of the Hardy-Dubios seven-point method by setting two FBG temperature sensors on the chest and armpits, and another between the two shoulder blades on the upper back. According to related papers, the breast temperature should be the highest and followed by the armpit temperature. The armpit temperature has almost no difference between the right and the left sides, whereas the upper back temperature should be the lowest. Hence, the data obtained from these five measuring points should yield the weighted average for the mean skin temperature.

The weighted coefficients of these five FBG sensors are C_1, C_2, C_3, C_4, and C_5 which are 0.0826, 0.3706, 0.3706, 0.0936, and 0.0826, respectively, according to the table.

In special cases, when some FBG sensors are broken, the weighted coefficients of the other sensors can be changed to generate the accurate body temperature. These cases can be categorized into the following conditions:

1. If a sensor placed on the breast or under the armpit is not working, while others work well, the temperature measured by the sensor on the symmetrical side of the broken sensor can be used because the temperature on the right breast is the same as that of the left breast, similar with the two armpits.

2. If a sensor on the upper back is not working, while others work well, the upper back temperature measurement can be disregarded. Data from the other sensors can then be calculated using new weighted coefficients C_1, C_2, C_3, and C_5 which are 0.0788, 0.4212, 0.4212, and 0.0788, respectively.

3. If the two sensors on the breasts are not working, while others work well, the data of the two sensors can be disregarded. The data from the other sensors can then be calculated using new weighted coefficients C_2, C_3, and C_4 which are 0.4361, 0.4361, and 0.1278, respectively.

4. If the two sensors under the armpits are not working, while others work well, the data of these two sensors can be disregarded. The data of others can then be calculate using new weighted coefficients C_1, C_4, and C_5 which are 0.3112, 0.3776, and 0.3112, respectively.

In considering these special situations, the weighted coefficients can be changed to guarantee the result of the experiments in real time even when some sensors are not working.

5. Conclusions

The FBG used in the experiment is encapsulated in unsaturated polymer resin. From the FBG sensors with 0.15 nm/°C sensitivity coefficient at the temperature of 33 °C–42 °C based on the improved packaging technology, the sensor's sensitivity coefficient is almost 15 times that of the bare FBG. Figure 5 shows an intelligent clothing sample which has implanted FBG sensors. The sensors are placed in the right chest, right armpit, left armpit, upper back, and left chest. In the experiment, the center wavelength data of the FBG sensors reflect the light first, prior to combining them with the sensitivity coefficients of the five FBG sensors. Afterward, the temperature measurements of the five points can be obtained through analysis and calculation using the formula. The temperature measured by the FBG error is ± 0.18 °C compared with the medical mercury thermometer, whereas the accuracy of the body

#164653 - $15.00 USD Received 14 Mar 2012; revised 30 Apr 2012; accepted 3 May 2012; published 9 May 2012
(C) 2012 OSA

temperature measurement is 0.1 °C. This accuracy meets the requirements of this study. The correlation is significant at the 0.01 level (two-tailed).

Using distributed FBG sensors to measure human body temperature, this study has acquired a sample of intelligent clothing and examined the heat transmission mechanism from many aspects, including the basic theory of human physiology, human thermal balance, and the theory of aerial heat transmission. A mathematic model of heat transmission for the human skin, the air, and clothing has also been established. This model provides the theoretical basis of human temperature measurement using intelligent clothing with distributed FBG sensors and demonstrates the planting of optical fiber grating into the clothing. This paper also proposes that the model, which is an improvement of the Hardy-Dubios seven-point method, confirms the measuring points of distributed FBG sensors in intelligent clothing. In the experiment, the difference between the body temperature measured by the distributed FBG sensors in intelligent clothing and the analog data of the thermal field has no statistical significance. Thus, the temperature measured by the distributed FBG sensors can be used to represent human body temperature in clinics.

Based on this, the researchers intend to expand research in intelligent clothing to cover the measuring and recording of real-time physiological information, such as human respiration, heartbeat, blood pressure, and other physiological signals. At the same time, some social trends, such as the growth of population aging and the increase of public awareness on health care, will change the form of pure hospital treatment into another form that combines the hospital, community, family, and individual. Thus, wearable biomedical instruments, which are non-intrusive, non-invasive, and continuously being monitored, will become important monitoring and diagnostic devices under this new type of medical model. These tools can detect and process physiological signals, extract signal characterization, transmit data, and have other basic functions. Life-intelligent clothing can monitor patients' suffering from heart disease or high blood pressure and the state of illness in a timely manner. Consequently, patients can ask for treatment and prevent complications and death. More importantly, intelligent clothing can record the physiological parameters of athletes, soldiers, astronauts, and others. These data can be used in the research on human physiology and health conditions. Life-intelligent clothing can then be applied widely in many fields, such as medical treatment, sports, military, and aeronautics.

Acknowledgments

This paper is supported by the National Natural Science Foundation of China (61177078, 60977059, 60877049) and the Specialized Research Fund for the Doctoral Program of Higher Education of China (20101201120001).

#164653 - $15.00 USD Received 14 Mar 2012; revised 30 Apr 2012; accepted 3 May 2012; published 9 May 2012
(C) 2012 OSA